Available online at www.sciencedirect.com
SCIENCE DIRECT
Polymer 47 (2006) 2849–2855
polymer
www.elsevier.com/locate/polymer

Effects of processing parameters on the preparation of nylon 6 nanocomposites

K. Yang, R. Ozisik *

Department of Materials Science and Engineering, Rensselaer Polytechnic Institute, Troy, NY 12180, USA

Received 20 September 2005; received in revised form 11 February 2006; accepted 13 February 2006
Available online 3 March 2006

Abstract

An experimental study was carried out to investigate the effects of the following parameters: (1) organic modifier and nylon 6 molecular weight, (2) processing conditions, and (3) pressure, with and without supercritical fluids, on the dispersion of clays for nylon 6/montmorillonite nanocomposites. A novel experimental setup was designed that physically separated the melting and mixing unit operations, and allowed control of the pressure using a pressure adjustable die. Exfoliated clay morphology was realized using a wide angle X-ray diffraction technique when both requirements of (1) selecting an organic modifier that was thermodynamically compatible with the polymer matrix and (2) applying sufficient degree of shear stress were fulfilled. Keeping the organic modifier constant, either longer residence time or the same level of shear stress did not improve the state of clay dispersion once a critical morphology was established. In the absence of supercritical fluids, pressure improved the clay delamination by reducing the free volume of the polymers and thereby increasing the interaction between the chains, and ultimately increasing the viscosity and, therefore, the level of wall shear stress. Using supercritical fluids such as either carbon dioxide or 1,1,1,2-tetrafluoroethane did not improve the clay dispersion for 95/5 N6-L/20A due to its role in increasing the free volume and decreasing the melt viscosity.

Keywords: Polymer processing; Nanocomposites; Supercritical fluids

1. Introduction

Polymer/clay nanocomposites have received widespread attention in academia, national laboratories, and industry [1]. Research in molecular props or pillars [2], organic intercalation [3], molecular dynamics and conformations in restricted geometries [4], mass transport of polymer chains into confined spaces [5], rheological properties [6] have all captured the interest. The promise of superior mechanical [7] and physical properties [8] has fostered extensive research and development programs with a trend towards commercialization. Montmorillonite, the clay of interest, has a platelet geometry with a thickness of ca. 1 nm and an aspect ratio of 250 to 500. Each layer is composed of two tetrahedral layers sandwiching an octahedral layer. There is a cation deficiency on the surface of the clay layers that is compensated by a sodium cation located between the layers. Since natural clays are hydrophilic, they are intercalated with short chain molecules to make it more 'compatible' with the host polymer, thereby making the clay organophilic. By diffusing host polymer chains into the layers of intercalated clay, the individual clay layers are separated or exfoliated. Over the years, researchers have investigated both polymerization and melt processing routes to polymer/clay nanocomposites preparation.

In the melt processing route, a suitable organic cation that is thermodynamically favorable with the host polymer is intercalated between the clay layers to promote clay dispersion [9,10]. Fornes et al. found that a high molecular weight polymer matrix leads to an improved clay dispersion rather than a low molecular weight due to its larger degree of transferable shear stress from the polymer matrix to the clay [11]. Processing conditions such as the process equipment that promotes high shear stress and shear rate were found to aid in clay dispersion along with the proper organic modifier [12,13].

Using clays as heterogeneous nucleating agents, supercritical fluids (SCF) such as carbon dioxide have been incorporated into polymer/clay nanocomposites to prepare microcellular foams with a high cell density and small cell size [14,15]. Although there are many studies that utilize a custom-made, continuous SCF assisted polymer processing setup, a comprehensive description of the equipment design is rare [15–17]. Also, the prevalent standard of using a die assembly with a replaceable capillary to control the die exit pressure is both time consuming and restricted to available capillary dies. Supercritical carbon dioxide have been used as a solvent for system that contains

* Corresponding author. Tel.: +1 518 276 6786; fax: +1 518 276 8554.
E-mail address: ozisik@rpi.edu (R. Ozisik).

0032-3861/$ - see front matter © 2006 Elsevier Ltd. All rights reserved.
doi:10.1016/j.polymer.2006.02.043

clays [18,19]. Studies on the effect of pressure on clay dispersion are limited [20] while a few attempted to elucidate the benefit of polymer intercalation into the clays with the aid of supercritical carbon dioxide [21,22].

Electron microscopy, X-ray diffraction, rheology, and mechanical and physical properties are the standard tools utilized to determine the degree of clay dispersion. Often, one method is combined with another to describe the state of dispersion both qualitatively and quantitatively. Transmission electron microscopy (TEM) provides a visual representation of the dispersion, and by performing image analysis of a number of micrographs, quantitative data can be obtained [23]. Property measurements represent bulk properties and in most cases, are not able to detect small differences in the state of dispersion. On the other hand, wide angle X-ray diffraction (WAXD) is suitable to distinguish quantitatively slight variations of the intercalated clay morphology. For these reasons, WAXD was selected as the primary technique for investigating the degree of clay exfoliation.

The objectives of this paper are to examine the effect of hydrostatic pressure, with and without SCF, on the degree of clay delamination, and to investigate the role of SCF, if any, on clay dispersion. While the prevalent choice of SCF is carbon dioxide due to its environmentally benign character and ease of handling, hydrofluorocarbons such as 1,1,1,2-tetrafluoroethane was utilized for the first time as SCF for polymer/clay nanocomposites. Carbon dioxide has received the most attention among supercritical fluids due to its low cost, non-toxic nature, and ease of handling while R-134a is a polar molecule commonly used in refrigeration and thermal insulation applications. The major highlights of findings are reported.

2. Experimental and process design

2.1. Materials

Two substantially different molecular weights of nylon 6 from BASF Performance Polymers were utilized: heat-stabilized injection molding grade (N6-L), and extrusion grade (N6-H). Nylon 6 pellets were used as received from vacuum-sealed bags without further drying. Montmorillonite with various or modifications (organoclays) were obtained from Southern Clay Products. Table 1 provides detailed characteristics of the polymers and clays employed in this study. For the processing of nylon 6/clay, a sterically hindered phenolic antioxidant, N,N′-hexamethylenebis(3,5-di-(*tert*)-butyl-4-hydroxyhydrocinnamamide), (Irganox 1098, Ciba Specialty Chemicals), was added in the amount of 0.2 wt% of the polymer to stabilize nylon 6. The two fluids utilized were carbon dioxide and 1,1,1,2-tetrafluoroethane (R-134a). Commercial carbon dioxide with 99.9% purity and compressed to 5.66 MPa was obtained from AWESCO, and R-134a was obtained from Honeywell.

Table 1
Characteristics of materials employed in this study

Material	Code used	Supplier	Specifications
Nylon 6	N6-L	Capron 8202HS	M_n[a] = 16,400 g/mol
Nylon 6	N6-H	Capron B135QP	M_n[a] = 29,300 g/mol
Organoclay	10A	Cloisite 10A	Dimethyl benzyl hydrogenated-tallow ammonium
Organoclay	20A	Cloisite 20A	Dimethyl bis(hydrogenated-tallow) ammonium
Organoclay	25A	Cloisite 25A	Dimethyl 2-ethylhexyl hydrogenated-tallow ammonium
Organoclay	30B	Cloisite 30B	Bis(2-hydroxyl-ethyl)methyl tallow ammonium

[a] Data from intrinsic viscosity measurements at 25 °C [36].

2.2. Setup and processing conditions

Fig. 1 gives a schematic of the overall process showing the unit operations of the upstream and downstream regions along with the locations of the pressure transducers, P/T. In the upstream region, the dry blended 95/5 nylon 6/clay, by weight percent, was fed to the twin screw extruder (ZSK30, Coperion Werner and Pfleiderer) with a screw diameter of 30 mm and a length-to-diameter ratio (L/D) of 45 [24]. The feedrate of the nylon 6/clay mixture was 14 kg/h, and the twin screw extruder was operated at 300 rpm. The feed zone barrel temperature was set at 220 °C, all barrels thereafter at 240 °C, and the die at 250 °C. The pellets produced were dried overnight at 80 °C prior to subsequent processing. In the downstream process, the nylon 6/clay nanocomposites were flood-fed to an extrusion line custom made by New Castle Industries composed of two single screw extruders in tandem. For the primary extruder, the temperature was set from the feeding zone to the die head as 180, 240, 240, and 260 °C, and the screw was rotated at 20 rpm. For the secondary extruder, barrel temperature was set at 240 °C, and the screw was rotated at 90 rpm. The pressure adjustable die was heated to 220 °C. The fluid was compressed to 21 MPa using a positive displacement syringe pump (260D, Isco), and metered at 1 mL/min to the injection valve that was positioned at the secondary single screw extruder. The melt and SCF were mixed using a distributive-type screw [25] and pumped to the breaker plate, and finally left the system via a pressure adjustable die. In addition, an internal mixer (Thermo Haake, PolyDrive R600) equipped with roller rotors and a net chamber volume of 69 mL was used to prepare nylon 6/clay mixtures. These were compared to mixtures prepared with the twin screw extruder (TSE). The nylon 6/clay mixture was dry blended initially and fed to the mixer. The rotor speed was 50 rpm, and mixing was performed at 240 °C for 6, 11, and 16 min.

2.3. Characterization

Extrudate samples of 1.5 mm thickness were prepared by compression molding for 1 min at 265 °C and then applying 34 MPa for 1 min. An amorphous PMMA holder was utilized for the organoclay powders. An X-ray diffractometer (XDS 2000, Scintag) equipped with a Ni-filtered Cu K_α (0.154 nm) radiation source and operated at 50 kV and 30 mA was used.

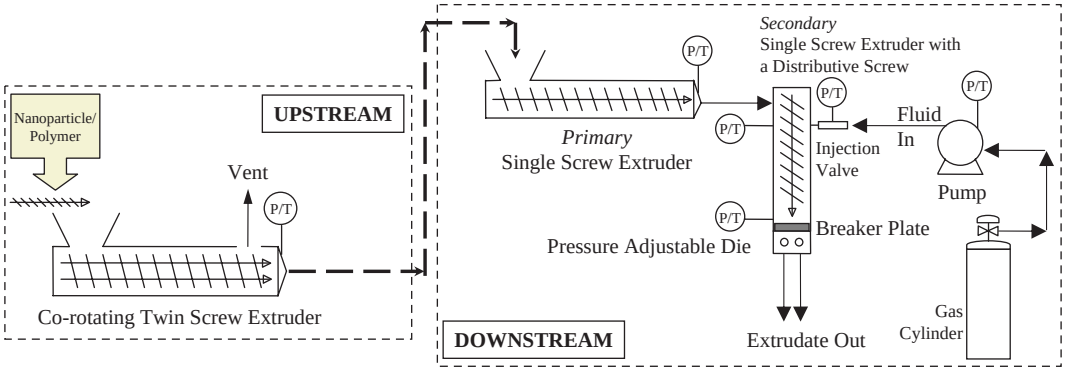

Fig. 1. Schematic of the overall process showing the upstream region where the nylon 6/clay nanocomposite was prepared using a twin screw extruder. The product was fed to the tandem extruder (downstream region) where it was injected with the fluid.

WAXD was used in reflection mode with 2θ ranging between 1 and 10° at 0.02°/mm increments. Samples for microscopy were prepared using an ultramicrotome (PowerTome XL, BAL-TEC RMC) equipped with a diamond knife, and then observed using a transmission electron microscope (CM12, Philips) at 120 kV.

3. Results and discussion

3.1. Effects of organic modifier and nylon 6 molecular weight

Fig. 2 shows WAXD patterns of pristine organoclays and 95/5 N6-L/organoclay nanocomposites. The first peak at the lowest diffraction angle, corresponds to the (001) of the montmorillonite basal layer spacing or *d*-spacing. Of the four different organoclays investigated, 30B showed the largest shift towards higher *d*-spacing as shown by Fig. 2(d). This was expected because the polar nature of nylon 6 is favorable with the hydroxyl groups of the quaternary alky ammonium in 30B. The effect of nylon 6 molecular weight on the clay dispersion is given in Fig. 3. When the organoclay was 20A, Fig. 3(a), the high molecular weight nylon 6 (N6-H), showed a *d*-spacing value of 3.53 nm compared to 1.96 nm for the low molecular weight nylon 6 (N6-L). The N6-L/30B showed a (001) peak at ca. $2\theta = 4.5°$ while N6-H/30B did not show any peaks

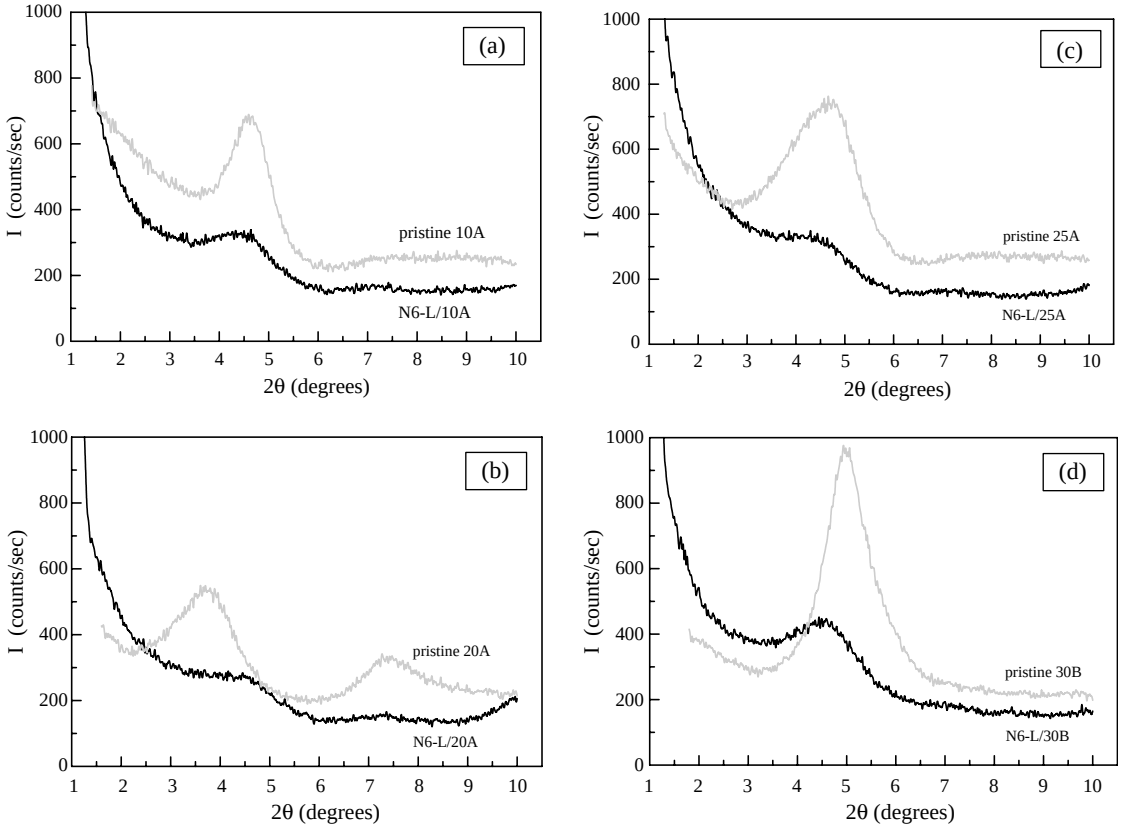

Fig. 2. WAXD patterns for pristine organoclay and 95/5 N6-L/organoclay nanocomposites formed from the quaternary alky ammonium organoclays: (a) 10A, (b) 20A, (c) 25A, and (d) 30B.

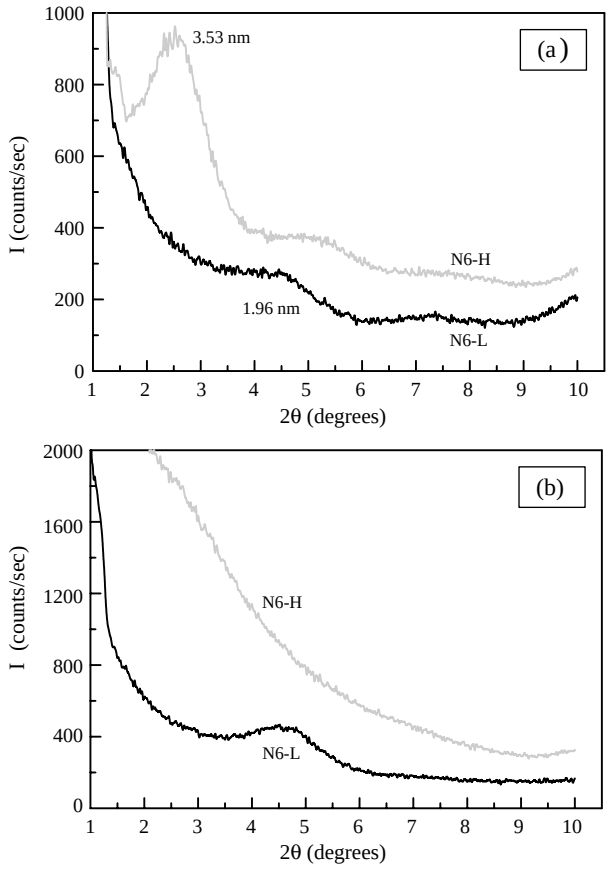

Fig. 3. WAXD patterns for 95/5 nylon 6/organoclay nanocomposites with varying nylon 6 molecular weights formed from oganoclays (a) 20A and (b) 30B. The curves are vertically offset for clarity.

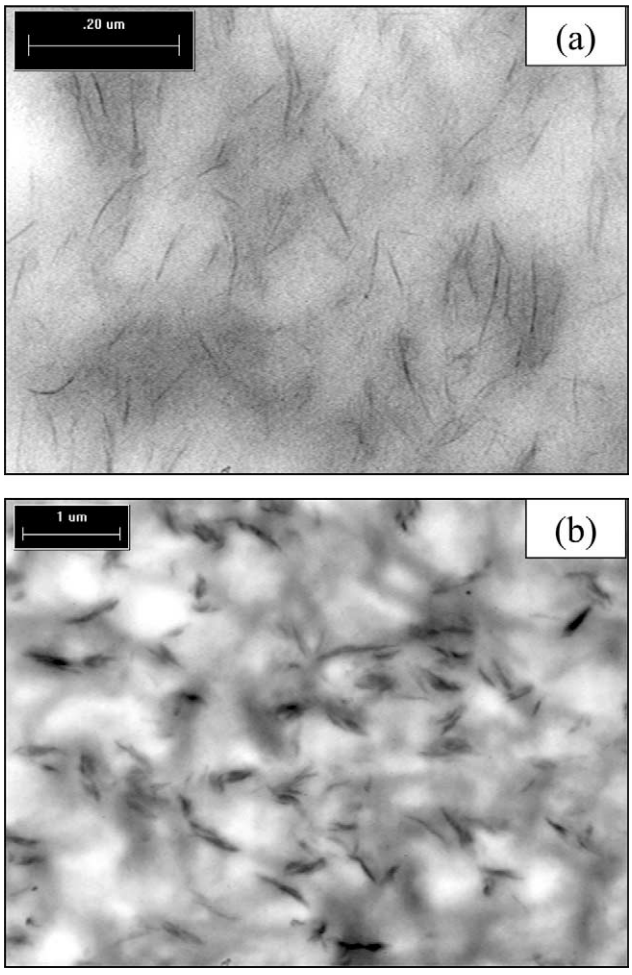

Fig. 4. TEM micrographs of (a) 95/5 N6-H/30B and (b) 95/5 N6-L/20A nanocomposites.

suggesting an exfoliated clay morphology. The polymer molecular weight plays a key role in clay dispersion because it enables the transfer of applied shear stress to the clays. Fornes et al. have shown using melt rheology that the shear stress, which is a function of viscosity and in turn is a function of molecular weight, plays a dominant role in clay dispersion [11].

Fig. 4(a) and (b) gives TEM micrographs of N6-H/30B and N6-L/20A, respectively. The TEM micrograph of N6-H/30B represents an exfoliated clay morphology where individual clay layers are detached from one another. The morphology of N6-L/20A shows tactoids, layers of clay. These two types represent two extremes of clay dispersion and are well correlated with WAXD patterns. Note that while WAXD can discern small deviations in morphology, it is more challenging to capture small deviations with TEM.

3.2. Effects of processing parameters

3.2.1. Type of mixer and distributive screw

An internal mixer and a twin screw extruder (TSE) were compared to determine their efficacy in clay dispersion. Also, the effect of residence time was investigated by varying either the mixing times or performing multiple passes. Two 95/5 N6-L/20A nanocomposites were prepared. The co-rotating TSE had two kneading block zones, while the internal mixer had roller-type rotors. Considering the two mixer setups and processing conditions, the TSE would be more efficient in dispersive and distributive mixings and the level of shear stress would be higher than the internal mixer. Fig. 5(a) shows this was indeed the case where a distinctive (001) peak was observed for the internal mixer with 16 min mixing time compared to a broadening and dampening of the (001) peak in samples prepared with the TSE after the third pass. The thermodynamics of clay dispersion is governed by the interaction between the organoclay and the polymer. Once a thermodynamically stable state is reached, no further improvement can be realized at a constant shear stress level. Therefore, exposing the sample to longer residence times does not have any effect on dispersion. This is shown by the results in Fig. 5(b) for the internal mixer and in Fig. 5(c) for the TSE. Fig. 5(b) and (c) demonstrate that the (001) peak does not change appreciably in position and size with residence time at constant shear stress level. Note that for multiple passes, pellets produced from the twin screw extruder were fed back to the hopper with appropriate amounts of thermal stabilizer (added to prevent nylon 6 degradation) to ensure a constant melt viscosity. The Saxton and Stratablend II [26,27] screws were also evaluated for their performance in improving clay

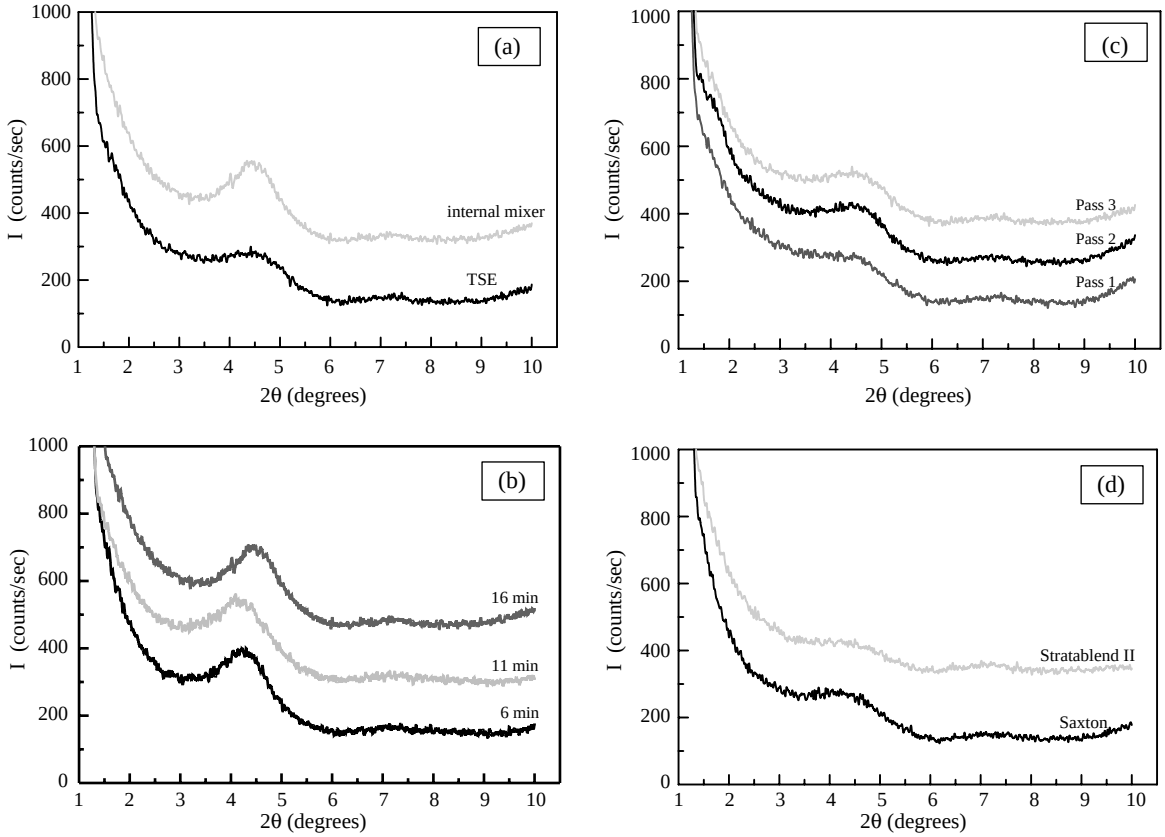

Fig. 5. WAXD patterns for 95/5 N6-L/20A nanocomposites prepared using (a) an internal mixer with 16 min mixing time and a twin screw extruder at the third pass, (b) an internal mixer for various mixing times, (c) a twin screw extruder with multiple passes, and (d) a tandem single screw extruders equipped with a torpedo breaker plate and a Stratablend II (2.00 MPa) or Saxton (2.14 MPa). The curves are vertically offset for clarity.

dispersion. Fig. 5(d) shows results for 95/5 N6-L/20A using a torpedo breaker plate. Considering both screws were designed specifically for distributive type of mixing, only a slight improvement in clay dispersion was realized for the Stratablend II compared to the Saxton due to its more efficient flow splitting and recombination. Screw design that take into account both dispersive and distributive mixing would have been more beneficial in clay dispersion than one alone.

3.2.2. Effects of pressure

The die head pressure of the secondary single screw extruder could be controlled by either varying the material property such as the nylon 6 molecular weight or processing parameters. The latter method was more effective in obtaining a wide range of pressure with minor adjustments. Of the many feasible processing parameters available, the use of a pressure adjustable die with the multi-capillary breaker plate with or without SCF provided the largest window of attainable pressure.

3.2.2.1. Without supercritical fluids. When pressure is applied to the polymer melt, the free volume decreases leading to an increase in the interaction between the polymer chains. The consequence is an increase in the melt viscosity [28–30] and hence, the polymer chain friction coefficient. At constant apparent shear rate, the wall shear stress is only a function of the viscosity. Therefore, pressure is proportional to the wall shear stress and the larger this value the better should be the clay dispersion. This was indeed the case for all four organoclays investigated for the 95/5 N6-L/organoclay system. Note that the die head pressure that was obtained when the die was partially opened was the maximum attainable steady state value. Fig. 6(a)–(d) shows WAXD patterns of nanocomposites when the die was fully or partially opened. For all four nanocomposites, although the area under the curve of the (001) peak at ca. $2\theta = 4.5°$ increased with pressure, there is an increase in the X-ray intensity at lower diffraction angles, suggesting a larger population of exfoliated clays.

3.2.2.2. With supercritical fluids. Carbon dioxide and R-134a were the two fluids utilized at their supercritical states. Table 2 provides the critical temperature, pressure, and density for these two fluids. Note that the processing conditions were well above the critical conditions for respective fluids and, therefore, the fluid phase was supercritical. Using the Lee/Kesler generalized-correlation model [31], the density of carbon dioxide and R-134a were calculated to be 0.2801 and 0.7118 g/cm^3, respectively. Taking into account their density difference and the polar nature of R-134a, the solubility parameter difference was expected to be high. This was indeed the case when carbon dioxide and R-134a solubility parameters were calculated as 4.85 and 7.71 MPa$^{1/2}$, respectively, using Materials Studio (Accelrys, Inc.). The nanocomposite system

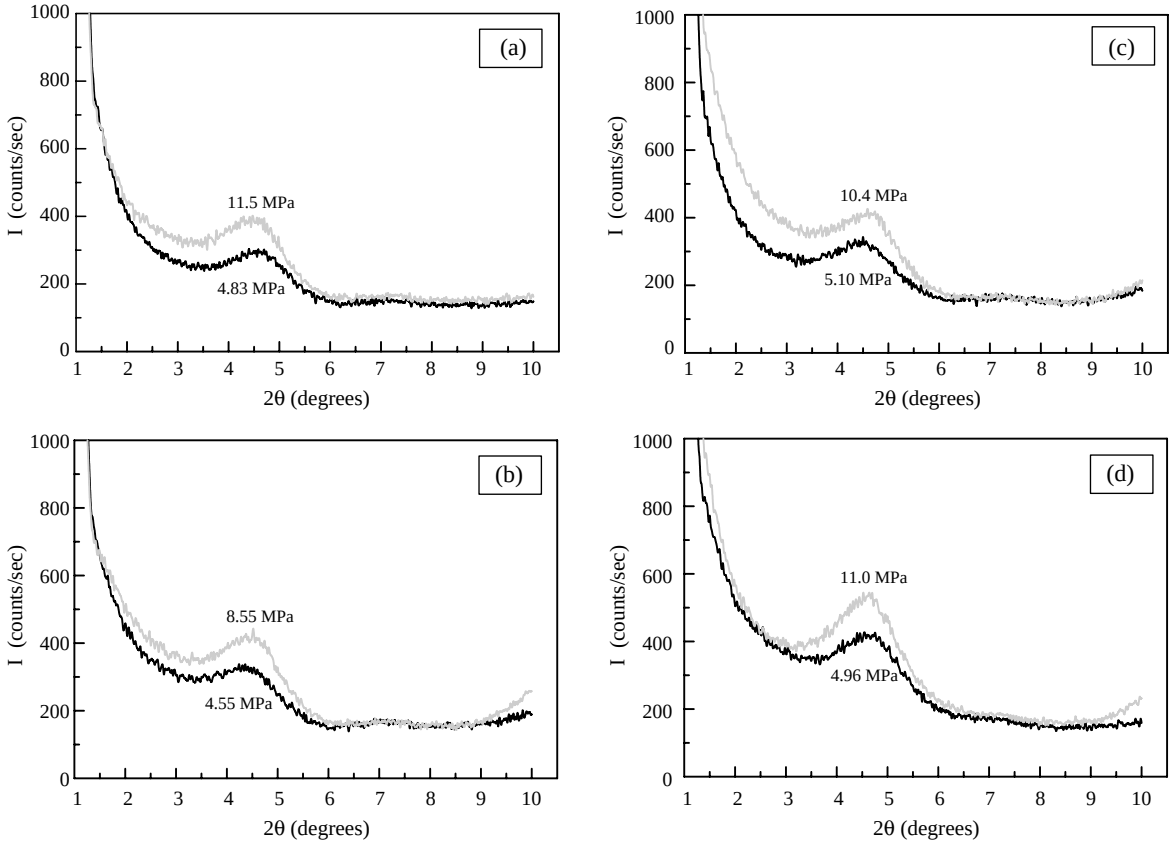

Fig. 6. WAXD patterns for 95/5 N6-L/organoclay nanocomposites prepared using a tandem single screw extruders equipped with a multi-capillary breaker plate and a Stratablend II screw: (a) 10A, (b) 20A, (c) 25A, and (d) 30B. The pressure values refer to the die head pressures of the secondary single screw extruder.

chosen for the SCF impregnation was 95/5 N6-L/20A which exhibited a clay dispersion that did not significantly change with additional processing, as previously discussed.

Fig. 7(a) gives WAXD patterns of the 95/5 N6-L/20A nanocomposites with and without supercritical carbon dioxide, $scCO_2$. Note that the pressure value without $scCO_2$ was obtained with a fully opened die, and with $scCO_2$, it was the maximum attainable steady state value. The clay dispersion became worse when $scCO_2$ was used. The area under the (001) peak at ca. $2\theta = 4.5°$ increased, and at lower diffraction angles the intensity decreased, reflecting more of an intercalated and less of an exfoliated clay morphology. When R-134a was utilized instead of $scCO_2$, the same general trend was observed as shown in Fig. 7(b).

The SCF results showed that pressure does not play a direct role in clay dispersion. Although the pressure attained was substantially higher when SCF was used, the clay dispersion was worse in nanocomposites with SCF than in nanocomposites without SCF. Using custom made rheological measuring devices, the addition of supercritical fluids to polymer was found to reduce the melt viscosity compared to the polymer alone [17,32,33]. The SCF acts as a low molecular solvent or has a plasticizing effect on the polymer by diluting the entangled polymer chain concentration. With an increase in the free volume as a result of solvent dissolution, both the chain mobility and the SCF diffusivity are enhanced. As the amount of the dissolved SCF increased, the free volume increased leading to a decrease in the melt viscosity. Both the dilution of the entangled polymer chain concentration and the free volume increase are the source of viscosity reduction [34,35]. The reduction in the melt viscosity leads to a decrease in the shear stress and results in an ineffective clay dispersion. Without SCF, pressure has a positive effect in increasing the polymer viscosity and hence, the magnitude of the load transfer from the polymer matrix to the clays increases.

4. Conclusions

A continuous, supercritical fluid assisted polymer processing setup was designed that separated the melting unit operation from the mixing, and utilized a novel, flow adjustable

Table 2
Critical conditions of fluids utilized [37]

Fluid	Chemical formula	Critical points		
		T_c (°C)	P_c (MPa)	ρ_c (g/cm^3)
Carbon dioxide	CO_2	31	7.38	0.4682
R-134a	CH_2FCF_3	101	4.06	0.5153

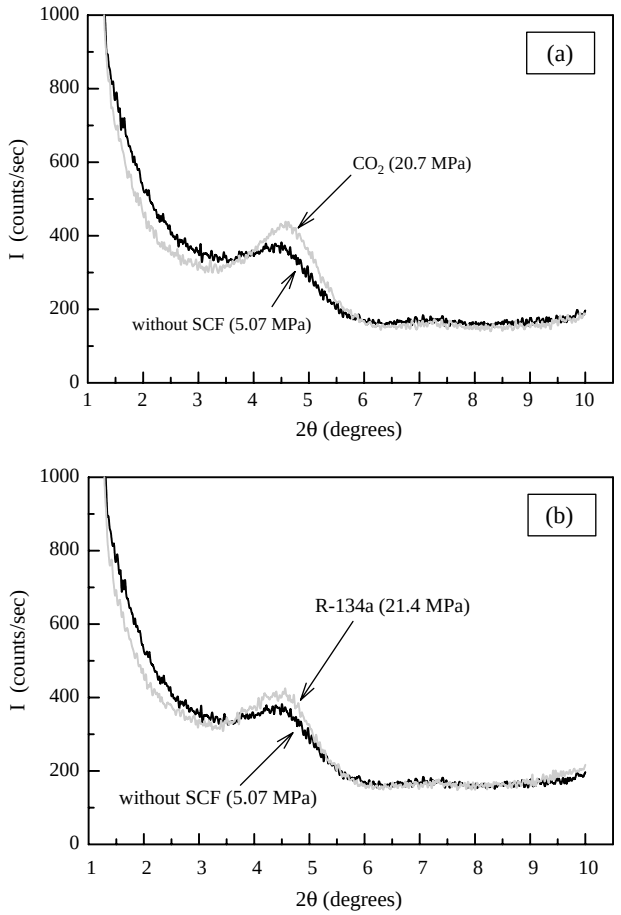

Fig. 7. WAXD patterns for 95/5 N6-L/20A nanocomposites prepared without and with supercritical fluid (a) carbon dioxide and (b) R-134a using a tandem single screw extruders equipped with a multi-capillary breaker plate and a Stratablend II screw.

die. Wide angle X-ray diffraction results showed that having a proper organic modifier was a necessary, but not a sufficient condition to obtain an exfoliated clay morphology. Along with the right chemistry, the level of shear stress transfer from the polymer matrix to the clays needs to be high, and one method of doing so was realized by using large molecular weight polymers. Results of various mixing times using an internal mixer and multiple passes in a twin screw extruder showed that longer residence time at constant shear stress did not alter the clay morphology. The effects of pressure, with and without supercritical fluids, on clay dispersion were investigated. Without supercritical fluids, pressure enhanced the clay dispersion because the polymer melt free volume decreased with pressure leading to an increase in the melt viscosity, and hence, the wall shear stress. Conversely, with the addition of supercritical fluids such as carbon dioxide or 1,1,1,2-tetrafluoroethane, the free volume increased and the melt viscosity decreased, two factors that do not contribute towards improving clay dispersion.

Acknowledgements

This work was supported by the Rensselaer Polytechnic Institute and partially funded from the National Science Foundation under grant number DMI-0500324. The authors would like to thank Southern Clay Products, BASF Performance Polymers, and Ciba Specialty Chemicals for generously donating the materials. Special thanks go to Dr E. Bruce Nauman for the use of the twin screw extruder.

References

[1] LeBaron PC, Wang Z, Pinnavaia TJ. Appl Clay Sci 1999;15(1–2):11–29.
[2] Pinnavaia TJ. Science 1983;220(4595):365–71.
[3] Barrer RM, MacLeod DM. Trans Faraday Soc 1955;51:1290–300.
[4] Hackett E, Manias E, Giannelis EP. J Chem Phys 1998;108(17):7410–5.
[5] Vaia RA, Jandt KD, Kramer EJ, Giannelis EP. Macromolecules 1995; 28(24):8080–5.
[6] Krishnamoorti R, Giannelis EP. Macromolecules 1997;30(14):4097–102.
[7] Kawasumi M, Hasegawa N, Kato M, Usuki A, Okada A. Macromolecules 1997;30(20):6333–8.
[8] Nyden MR, Gilman JW. Comput Theor Polym Sci 1997;7(3/4):191–8.
[9] Fornes TD, Yoon PJ, Hunter DL, Keskkula H, Paul DR. Polymer 2002; 43(22):5915–33.
[10] Fornes TD, Hunter DL, Paul DR. Macromolecules 2004;37(5):1793–8.
[11] Fornes TD, Yoon PJ, Keskkula H, Paul DR. Polymer 2001;42(25): 9929–40.
[12] Cho JW, Paul DR. Polymer 2001;42(3):1083–94.
[13] Dennis HD, Hunter DL, Chang D, Kim S, White JL, Cho JW, et al. Polymer 2001;42(23):9513–22.
[14] Okamoto M, Nam PH, Maiti P, Kotaka T, Nakayama T, Takada M, et al. Nano Lett 2001;1(9):503–5.
[15] Han X, Koelling KW, Tomasko DL, Lee LJ. Polym Eng Sci 2002;42(11): 2094–106.
[16] Park CB. PhD dissertation. Massachusetts Institute of Technology; 1993.
[17] Lee MH, Park CB, Tzoganakis C. Polym Eng Sci 1999;39(1):99–109.
[18] Ishii R, Wada H, Ooi K. Chem Commun 1998;(16):1705–6.
[19] Zerda AS, Caskey TC, Lesser AJ. Macromolecules 2003;36(5):1603–8.
[20] Fasulo PD, Rodgers WR, Ottaviani RA. Polym Eng Sci 2004;44(6): 1036–45.
[21] Garcia-Leiner M, Lesser AJ. PMSE Prepr 2003;88:92–3.
[22] Zhao Q, Samulski ET. Macromolecules 2003;36(19):6967–9.
[23] Fornes TD, Paul DR. Polymer 2003;44(17):4993–5013.
[24] Yang K, Lee SH, Oh JM. Polym Eng Sci 1999;39(9):1667–77.
[25] Rauwendaal C. Plast World 1997;55(5):38–42.
[26] Saxton RL. US Patent 3006029; 1961.
[27] Womer TW, Lepore BL. US Patent 6488399 B1; 2002.
[28] Maxwell B, Jung A. Mod Plast 1957;25:174.
[29] Westover RF. SPE Trans 1961;1(40):14–20.
[30] Kiran E, Brennecke JF, editors. Supercritical fluid engineering science fundamentals and applications, vol. 514. Washington DC: American Chemical Society; 1993. p. 104.
[31] Lee BI, Kesler MG. AIChE J 1975;21(3):510–27.
[32] Kwag C. PhD dissertation. Wayne State University; 1998.
[33] Royer JR, Gay YJ, Adam M, DeSimone JM, Khan SA. Polymer 2002; 43(8):2375–83.
[34] Gerhardt LJ, Manke CW, Gulari E. J Polym Sci, B: Polym Phys 1997; 35(3):523–34.
[35] Garg A, Gulari E, Manke CW. Macromolecules 1994;27(20):5643–53.
[36] Oshniski AJ, Keskkula H, Paul DR. Polymer 1996;37(22):4891–907.
[37] Smith JM, Van Ness HC, Abbott MM. Introduction to chemical thermodynamics. 6th ed. Singapore: McGraw-Hill; 2001 p. 655.